# Analysis of One-Dimensional Thermal Conductivity in a Copper Rod

Zavier Kamath, Josie Rose, Vika Vorona

The Ohio State University, Department of Physics, Columbus, OH 43210

**Abstract**

This experiment serves as a verification of expected one-dimensional heat conduction behavior following the heat equation with modifications to include radial loss and time-changing boundary conditions. We compare numerical solutions to the modified heat equation for the temperature along the rod at three different times across three runs of the experiment to measured data and find reasonable agreement with $\chi^2 = 1.43$ on average.

## 1 Introduction

Heat transfer is accomplished by three primary mechanisms: conduction, convection, and radiation. Conduction is the transmission of heat directly through a substance, convection is the transmission of heat by fluid motion, and radiation is the transmission of energy by electromagnetic waves [1]. In this experiment, we are interested in conduction.

Heat conduction is the characteristic form of energy transfer in solids where thermal energy moves from high to low temperature through vibration of molecules and, for metals, through free electrons [2]. The heat conduction behavior of a highly efficient heat-transferring copper rod is found in this experiment by measuring the temperature along its length over time. The characteristic behavior of heat conduction along a one-dimensional rod displays a simple manifestation of an object undergoing behavior governed by a differential equation (Eq. (12)).

Fourier's law, outlined in Appendix A, explains that heat transfer is proportional to the temperature gradient in a material. Materials of high conductivity such as copper conduct heat quickly, which creates steep temperature gradients [3]. Insulation reduces environmental effects, but we will still take these effects into account in this experiment.

In this experiment we establish a steady-state gradient in a copper rod, then apply boundary conditions to each side and measure the temperature along the rod. We then compare our experimental temperature measurements over time to numerical solutions to the modified heat transfer differential equation (Eq. (2)) with modified boundary conditions and find reasonable agreement.

# 2 Theory

Consider a small cylindrical element of cross-sectional area $A$, length $\Delta x$, and temperature difference $\Delta T$ across its ends (Fig. 1). Let $\phi(x,t)$ be the heat flux (heat flow rate through an area) at position $x$ and time $t$. Assume that this rod is one-dimensional and currently has minimal radiative losses from the lateral sides (such that the only mechanism for heat transfer is conduction between atoms in the rod). We will consider radiative losses the next section.

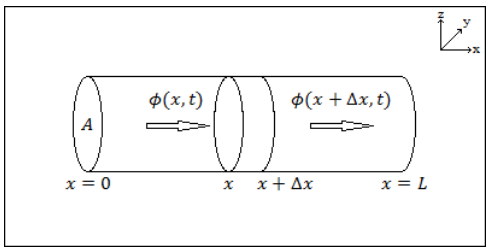


Figure 1: Source: Ref. [4]. Heat flow through a differential cylindrical element.

Following the derivation in Appendix A (and shifting $\mathrm{U} = \mathrm{T} - \mathrm{T_c}$ with $\mathrm{T_c}$ the temperature of the cold water) we obtain the 1D heat equation:

$$\boxed{\frac{\partial U}{\partial t} = \alpha^2 \frac{\partial^2 U}{\partial x^2}} \tag{1}$$

where $\alpha^2 \equiv \frac{k}{\rho c}$ is the thermal diffusivity. An important assumption for this solution is that $\rho$, $c$, and $k$ (density, specific heat, and thermal conductivity of the rod material respectively) do not change with $T$.

## 2.1 Heat Equation Fundamentals (Follows Ref. [5])

By taking radial heat loss into account, we can modify Eq. (12):

$$\frac{\partial U}{\partial t} = \alpha^2 \frac{\partial^2 U}{\partial x^2} - c(U - U_r) \tag{2}$$

where $U_r$ is the room temperature, and $c$ is a constant (different from specific heat) that quantifies the radial heat loss through the sides of the cylinder. An assumption is that $c$ does not change with $T$.

### 2.1.1 Steady-State Solutions

**Without Radial Loss ($c = 0$):** Reduces to classic heat equation with straight line solution:

$$U_{ss}(x) = Kx, \;\; K = \frac{T_h - T_c}{L} \tag{3}$$

$T_h$ and $T_c$ are the temperatures at $x = L$ and $x = 0$ respectively. These temperatures are the boundary conditions that we choose to set up different steady-state solutions. This solution is derived in Ref. [5]. This steady state solution is the initial condition for our transient phase.

**With Radial Loss ($c \neq 0$):** Requires solving Eq.(2) with $\frac{\partial U}{\partial t} = 0$ yielding exponential steady-state solutions of the form $U_{ss}(x) = Ae^{sx} + Be^{-sx} + U_r$, where $s \equiv \sqrt{c}/\alpha$. The detailed derivation and the exact forms of A and B are given in Ref. [5]. This solution is used to determine the errors associated with each thermocouple measurement (explained further in Appendix B).

### 2.1.2 Time-Dependent Solutions

To solve the $t \neq 0$ case, we make a change of variables: $\tilde{U}(x,t) = U(x,t) - U_e(x)$ to solve Eq. (2) where $U_e(x)$ is the steady state solution where both sides are cooled to the lower temperature. The solution takes the form:

$$\tilde{U}(x,t) = \sum_{n=1}^{\infty} g_n \sin(\gamma_n x) e^{-(\alpha^2\gamma_n^2 + c)t} \tag{4}$$

where $\gamma_n$ incorporates both the chosen boundary conditions and radial loss effects. The detailed derivation of Eq. (4) and exact form of $g_n$ and $\gamma_n$ are given in Ref. [5]. These solutions are used to find the best fit parameters which are then plugged in to the numerical solutions to Eq. 2 with modified boundary conditions (explained further in Appendix C).

### 2.1.3 Numerical Solutions

The original analytical solutions (Eq. (4)) to the modified heat equation do not take into account two things:

1. The thermocouples may not start and end at the ends of the rod (there could be extra length on each end)
2. The hot-end boundary condition does not change instantaneously (in reality it changes exponentially)

We can modify the analytical solution to account for condition 1 and use this solution to fit for the extra lengths on each end. To account for condition 2, we will need to use a changing boundary condition, and numerically solve the differential equation (Eq. (2)).

# 3 Experimental Methods

Following Ref. [6], we take a foam-insulated copper rod of 0.75-inch diameter and subject it to a temperature gradient by having hot water flow along one end and cold water flow along the other. After a linear steady-state gradient is produced and the temperature of the rod is no longer changing, cold water is run on both ends, and temperature readings are made at 11 equally spaced points along the rod (3 inches between each thermocouple). This setup allows both steady-state and transient heat conduction to be studied, providing insight into how rapidly and uniformly copper distributes thermal energy. We take data for at least 30 minutes, then repeat this process three times (each with a different hot water temperature).

We heat the hot water with an electric heater (the temperature is selected by voltage of the heater). Cold water flows from a sink to the side tubes of the rod (the rod is shaped

like an H with tubes on the sides to allow water flow). The hot side water is trapped and heated. When it is time to let cold water flow on both sides, the water is allowed to flow free and the heater is turned off.

The errors in temperature are determined by comparing the fitted steady-state distributions to the experimental data for each run and averaging the RMSE. We also consider the errors in position of the thermocouples along the rod (discussed further in the data analysis section).

# 4 Data Analysis

Numerical differential equation solving methods were used to find the theoretical distributions for the temperature along the length of a copper rod subject to the boundary conditions described in Experimental Methods. $\alpha = 0.414 \frac{\text{inches}}{\sqrt{\text{sec}}}$ was used for the copper rod in this experiment [6]. Room temperature was assumed to be 22°C. The values for other parameters used, such as the extra lengths of the rod on each end, the radial loss coefficient, and the cold water temperature are given in Appendix C. The hot water temperature was found by interpolating from the cold temperature at t=0 along the full length of the rod. As mentioned in the theory section, we assume that the boundary condition on the hot end starts at $T_h$ (the temperature of the hot water), and exponentially decays over time. The exponential decay constant k (from $T_h = T_{h,0} e^{-kt}$) was fitted for each run while computing the numerical solution. The k values found were $0.18 \pm 0.29$ 1/s, $0.21 \pm 0.31$ 1/s, and $0.23 \pm 0.28$ 1/s for run 1, run 2, and run 3 respectively.

We assume an error in thermocouple position of 0.5 in. [6]. The methods for obtaining the thermocouple temperature errors (as well as a table containing the error values) are given in Appendix C. The numerical solutions were plotted with experimental data on top for 3 selected times for each of the 3 runs. The times (4, 7, and 13 minutes) were chosen to show the heat decay behavior over time. Results are shown in Fig. 2 with reduced $\chi^2$ values reported for each fit.

# 5 Results

The reduced $\chi^2$ values for the fits in Fig. 2 have a distribution of $\chi^2 = 1.43 \pm 1.27$. The average is within the 95% confidence interval for reduced $\chi^2$ values, but only for less than $1\sigma$ of the distribution. This implies that some of our numerical solutions are overfit, and some are underfit. To understand why run 1 may be underfit (i.e. does not follow the theoretically predicted distribution) and to view the raw thermocouple data, see Appendix D. It is also possible that we overestimated the errors in position, which resulted in some of the distributions being overfit. By qualitative visual inspection, we can see that the experimental data points do generally trace out the same shape as the theoretical fits.

# 6 Conclusions

The characteristic behavior of heat conduction along a rod displays a simple manifestation of an object undergoing behavior governed by a differential equation (Eq. (12)). In this

experiment, we measured this manifestation by recording the temperature along a copper rod that is subject to boundary conditions over time. We considered an extension to the basic heat equation that accounts for radial loss and an exponentially decreasing hot-end temperature. Our models found reasonable agreement with the measured data ($\chi^2 = 1.43 \pm 1.27$), verifying that heat conduction behavior can be predicted reliably if system parameters are well understood.

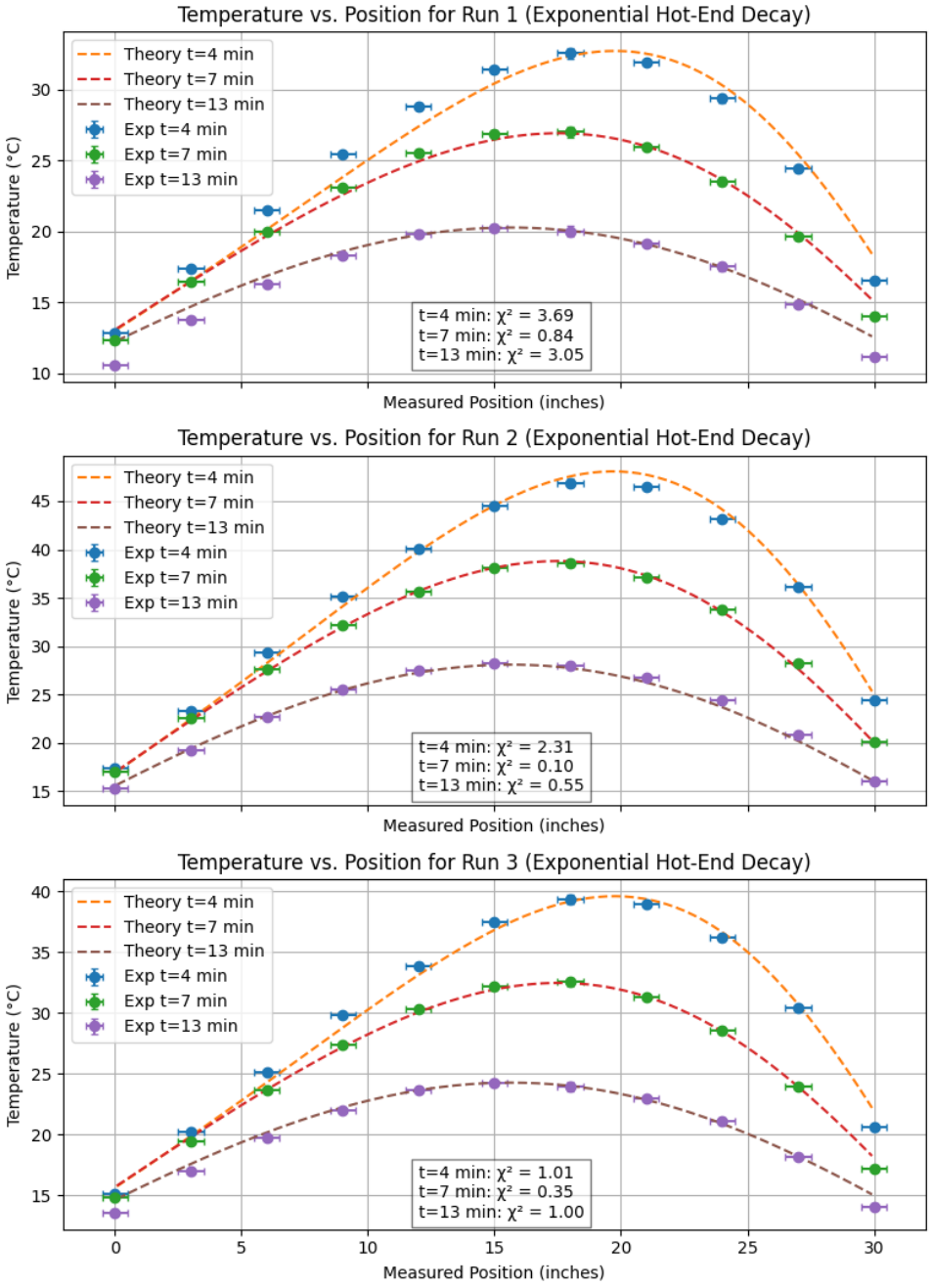


Figure 2: Experimental data points with errors plotted on top of numerical solutions for the modified heat equation with modified hot-end boundary conditions. Reduced $\chi^2$ values computed with x and y errors. Temperature errors are included, but may be too small to see.

# Appendix A: Derivation of the Heat Equation (following Ref. [7])

Consider the cylindrical element in the theory section.

**Energy Conservation:** The net heat energy entering the element is:

$$\Delta H = H_{in} - H_{out} \tag{5}$$

Where $H_{in}$ occurs at $x$ and $H_{out}$ occurs at $x + \Delta x$.

**Fourier's Law:** The heat flux $\phi(x,t)$ is proportional to the negative partial derivative of temperature w.r.t. x:

$$A\phi(x,t) = -kA\frac{\partial T}{\partial x},\ \ \phi(x,t) = \frac{H(x,t)}{A\Delta t} \tag{6}$$

where $k$ is the thermal conductivity.

**Combining (5) and (6):** Consider the rate of heat change during a small time $\Delta t$ between two points $\Delta x$ and $x + \Delta x$:

$$\frac{\Delta H}{\Delta t} = -kA\left[\frac{\partial T}{\partial x}\Big|_x - \frac{\partial T}{\partial x}\Big|_{x+\Delta x}\right] \tag{7}$$

**Remember this equation from Thermodynamics:**

$$\Delta H = mc\Delta T,\ \ m = \rho A\Delta x \tag{8}$$

Where $m$ is the mass of the rod (which can be found by multiplying the density times the area times the element distance) and $c$ is the specific heat of the material of the rod.

**Combining (7) and (8):**

$$\frac{\rho Ac\Delta x\Delta T}{\Delta t} = -kA\left[\frac{\partial T}{\partial x}\Big|_x - \frac{\partial T}{\partial x}\Big|_{x+\Delta x}\right] \tag{9}$$

Rearranging:

$$\frac{\Delta T}{\Delta t} = \frac{k}{\rho c}\left(\frac{\frac{\partial T}{\partial x}\Big|_{x+\Delta x} - \frac{\partial T}{\partial x}\Big|_x}{\Delta x}\right) \tag{10}$$

Taking the limit as $\Delta x$ and $\Delta t \Longrightarrow 0$ and noticing that the R.H.S. contains the limit definition of the derivative of the partial derivative w.r.t. x of T:

$$\frac{\partial T}{\partial t} = \frac{k}{\rho c}\frac{\partial^2 T}{\partial x^2} \tag{11}$$

If we substitute $U(x,t) = T(x,t) - T(x=0)$ the final result is the 1D heat equation:

$$\boxed{\frac{\partial U}{\partial t} = \alpha^2\frac{\partial^2 U}{\partial x^2}} \tag{12}$$

where $\alpha^2 \equiv \frac{k}{\rho c}$ is the thermal diffusivity. An important assumption for this solution is that $\rho$, $c$, and $k$ do not change with $T$.

# Appendix B: Thermocouple Error Calculation

To compute the error associated with each thermocouple, we used the exponential steady-state model from section steady-state solutions to fit the steady-state data (T versus x at t=0) for each run (shown in Fig. 3).

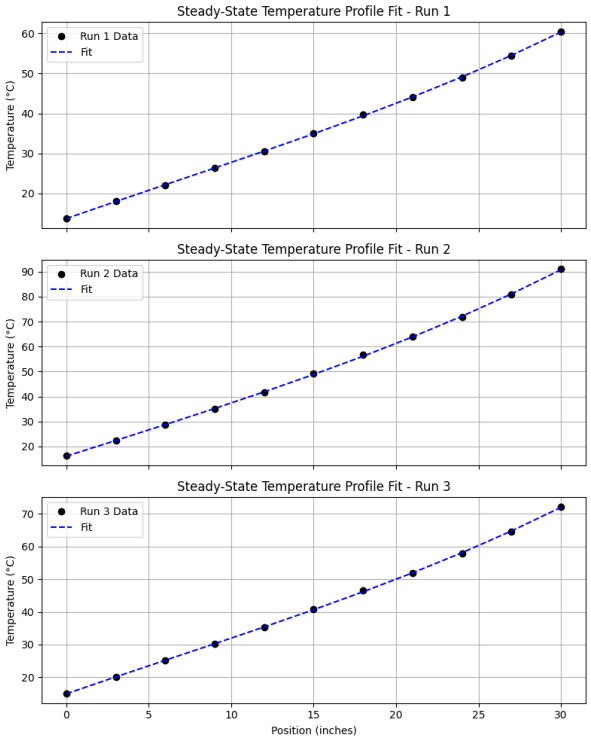


Figure 3: Steady-state gradient fit for each run. Fit follows the solution in the steady-state solutions section that includes radial loss.

We then compute the errors for each thermocouple as the average RMSE between the experimental data and the model fits for all runs. These errors are given in Table 1.

| Thermocouple | Average Error (°C) |
|---|---|
| 1 | 0.084 |
| 2 | 0.042 |
| 3 | 0.102 |
| 4 | 0.042 |
| 5 | 0.238 |
| 6 | 0.222 |
| 7 | 0.389 |
| 8 | 0.017 |
| 9 | 0.299 |
| 10 | 0.213 |
| 11 | 0.206 |

Table 1: Average error for each thermocouple

# Appendix C: Discussion of Parameter Fitting from Analytical Model

The analytical fit plots for each run are shown in Fig. 4, with the found fit parameters given in Table 2.

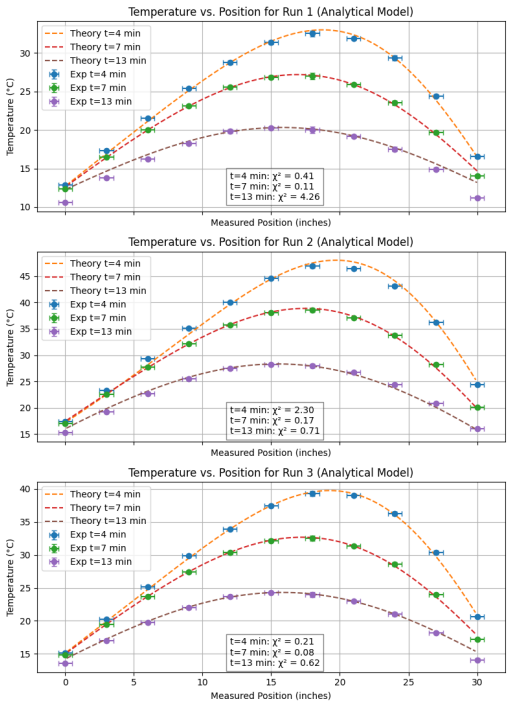


Figure 4: Experimental data points with errors plotted on top of analytical solutions for the modified heat equation (regular boundary conditions). $\chi^2$ computed with x and y errors.

It is interesting to note that the analytical solutions fit the data significantly better than the numerical approximations to the modified heat equation with modified boundary conditions. Even though this is true, we use the numerical solutions for the main analysis in this work because they should (in theory) be a closer approximation to the true distribution (because we know that the boundary condition should not change immediately). Regardless, these analytical fits provide us with fit parameters to use in our numerical approximations. These fit parameter values should not be taken exactly, due to the fundamental difference in the models (hot-end temperature instantaneous change versus exponential decay). Instead, they provide a good starting point to search for the parameters to use in the numerical approximation.

| Run | extra_left (inches) | T_cold (°C) | extra_right (inches) | c |
|---|---|---|---|---|
| **Run 1** | $0.75 \pm 3.54$ | $11.64 \pm 4.80$ | $1.79 \pm 5.18$ | $1.59 \times 10^{-18}$ |
| **Run 2** | $3.60 \pm 2.38$ | $11.11 \pm 3.55$ | $3.03 \pm 1.61$ | $1.72 \times 10^{-17}$ |
| **Run 3** | $1.61 \pm 5.18$ | $12.54 \pm 7.94$ | $2.45 \pm 5.75$ | $7.52 \times 10^{-29}$ |
| **Average** | 1.99 | 11.76 | 2.42 | $6.26 \times 10^{-18}$ |
| **Used Value** | 3 | 11.5 | 3 | 4.4e-5 |

Table 2: Fitted analytical model parameters and values used in numerical simulations. The c values had associated errors in the $10^{-4}$ range. extra_left and extra_right are the extra distances on the left and right sides of the rods past the first and last thermocouples.

After manually searching for the best parameters (the parameters that minimized the $\chi^2$ values in Fig. 2), we found the values in the "Used Value" row. The c value that was used was given by Dr. Farell in Ref. [8] and computed using Fourier's law and the cylindrical model in the theory section.

# Appendix D: Discussion of Data Behavior

Fig. 5 shows the raw temperature versus time data for each thermocouple on each run. We can examine it to see that run 1 had some extra noise compared to the other runs, especially in the thermocouple closest to the cold water. This could indicate that there were fluctuations in the cold water temperature that we did not account for. Considering the fact that we were taking the cold water from a sink that has unknown temperature stabilization systems, it is not surprising to expect that the cold water temperature could change drastically throughout a run. This behavior may explain the higher $\chi^2$ values in run 1 of Fig. 2.

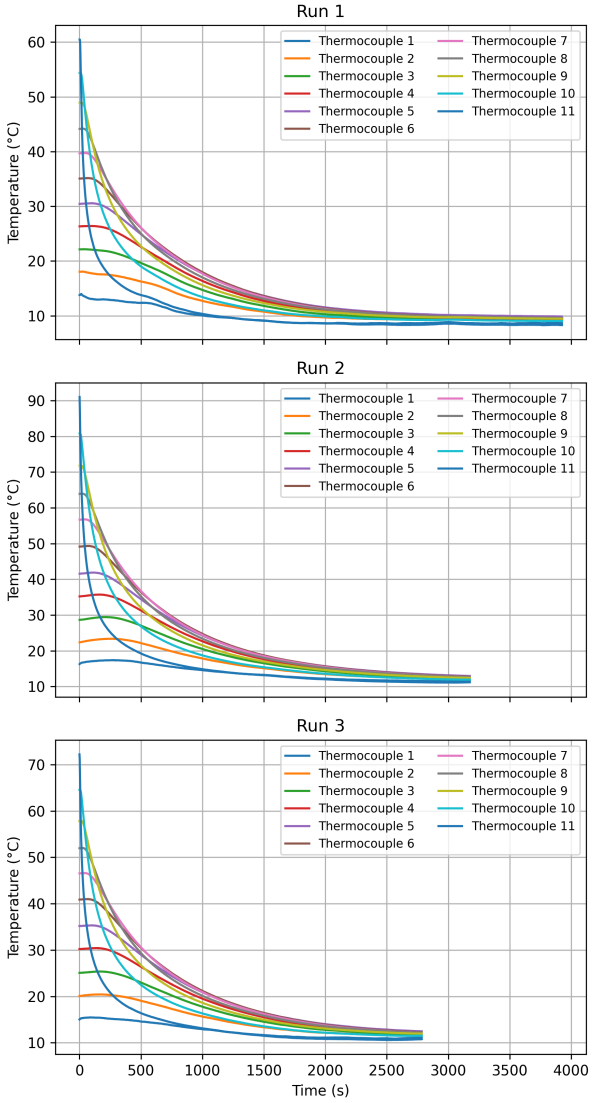


Figure 5: Raw thermocouple data. Displays the temperature of each thermocouple over time for each run of the experiment. Thermocouple 11 is the closest to the hot end and Thermocouple 1 is closest to the cold end.

# References


[1] NOAA, *The transfer of heat energy*, 2023.

[2] Energy Education, *Heat transfer mechanisms*, 2023.

[3] BYJU'S, *Fourier's law - formula, derivation, definition, equation*, 2019.

[4] J. Molina, *Derivation of the heat equation*, 2012. Accessed: 2025-02-18.

[5] D. J. Gauthier and J. Martin, *Heat conduction along a thin rod with radial heat loss*, . Unpublished manuscript.

[6] Carmen/Canvas, *Experiment in one-dimensional thermal conductivity with boundary conditions*, 2025.

[7] Carmen/Canvas, *Simple derivation of the heat equation*, 2025.

[8] D. M. Farrell, "Radial loss constant calculation." Email correspondence, Mar., 2025. Email sent to Zavier Kamath.